Development 133, 1045-1057 (2006) doi:10.1242/dev.02278

NF-κB transmits Eda A1/EdaR signalling to activate Shh and cyclin D1 expression, and controls post-initiation hair placode down growth

Ruth Schmidt-Ullrich[1,*], Desmond J. Tobin[2], Diana Lenhard[1], Pascal Schneider[3], Ralf Paus[4] and Claus Scheidereit[1]

A novel function of NF-κB in the development of most ectodermal appendages, including two types of murine pelage hair follicles, was detected in a mouse model with suppressed NF-κB activity ($c^{I\kappa B\alpha\Delta N}$). However, the developmental processes regulated by NF-κB in hair follicles has remained unknown. Furthermore, the similarity between the phenotypes of $c^{I\kappa BA\Delta N}$ mice and mice deficient in Eda A1 (*tabby*) or its receptor EdaR (*downless*) raised the issue of whether in vivo NF-κB regulates or is regulated by these novel TNF family members. We now demonstrate that epidermal NF-κB activity is first observed in placodes of primary guard hair follicles at day E14.5, and that in vivo NF-κB signalling is activated downstream of Eda A1 and EdaR. Importantly, ectopic signals which activate NF-κB can also stimulate guard hair placode formation, suggesting a crucial role for NF-κB in placode development. In *downless* and $c^{I\kappa B\alpha\Delta N}$ mice, placodes start to develop, but rapidly abort in the absence of EdaR/NF-κB signalling. We show that NF-κB activation is essential for induction of Shh and cyclin D1 expression and subsequent placode down growth. However, cyclin D1 induction appears to be indirectly regulated by NF-κB, probably via Shh and Wnt. The strongly decreased number of hair follicles observed in $c^{I\kappa B\alpha\Delta N}$ mice compared with *tabby* mice, indicates that additional signals, such as TROY, must regulate NF-κB activity in specific hair follicle subtypes.

KEY WORDS: Hair follicle, NF-κB, Eda A1, EdaR, TNF, Skin, Cyclin D1, Shh, TROY (Tnfrsf19), Mouse

INTRODUCTION

Well-described cellular and physiological functions of the transcription factor NF-κB, determined via cell culture assays and various knockout and transgenic mouse models, include apoptosis, cell proliferation, and the adaptive and innate immune responses (Hayden and Ghosh, 2004; Karin and Ben-Neriah, 2000). An essential function of NF-κB in the development of secondary peripheral lymph nodes, Peyer's patches and ectodermal appendages (e.g. hair follicles, teeth, and exocrine glands) was first demonstrated in the $c^{I\kappa B\alpha\Delta N}$ mouse model, in which the human transdominant NF-κB inhibitor IκBαΔN was ubiquitously expressed, using in-frame integration into the β-catenin locus (Ohazama et al., 2004b; Schmidt-Ullrich et al., 2001).

Mice with suppressed NF-κB activity ($c^{I\kappa B\alpha\Delta N}$) shared an identical epidermal phenotype with *tabby* (mutant Eda A1, ectodysplasin A1), *downless* (mutant EdaR, ectodysplasin receptor), *crinkled* (mutant EDARADD) and Traf6-deficient mice. This phenotype is analogous to the human hereditary disease HED (hypohidrotic ectodermal dysplasia) (Schmidt-Ullrich et al., 2001), and manifests itself in severe defects of hair, molar tooth and exocrine gland development (Ohazama et al., 2004b; Schmidt-Ullrich et al., 2001). Eda A1 and EdaR belong to the tumour necrosis factor (TNF) multigene family of ligands and receptors respectively, and are able to activate NF-κB and the JNK/AP1 pathway in vitro (Aggarwal, 2003; Headon and Overbeek, 1999; Kumar et al., 2001; Mikkola et al., 1999; Yan et al., 2000). The EdaR-associated death domain protein, EDARADD, interacts with the death domain of EdaR, implicating a link to downstream signal cascades including Traf6 and IKK/NF-κB activation (Headon et al., 2001; Naito et al., 2002).

Epidermal appendages, including hair follicles, develop through complex reciprocal signalling interactions between the ectoderm and the underlying mesoderm (Hardy, 1992). The fur coat of mice is composed of four types of pelage hair follicles: the long guard or tylotrich hairs (2-10%), with large bulbs and sebaceous glands; the shorter and thinner intermediate awl and auchene (25-30%); and the downy zigzag hairs (60-70%) (Sundberg, 1994). Pelage hair develops in three consecutive waves, starting at embryonic stage E14.5 for guard hairs (primary hairs), followed by the intermediate hairs at E16-E17 and zigzag hair development around birth (secondary hairs) (for reviews, see Philpott and Paus, 1998; Schmidt-Ullrich and Paus, 2005).

Hair follicle development is divided into eight morphologically distinct stages (Schmidt-Ullrich and Paus, 2005). The earliest visible morphological signs of hair development are placodes (stage 1), groups of rearranged keratinocytes in the epidermis, which begin to divide and penetrate into the underlying mesoderm (stages 1-4), eventually giving rise to different parts of the hair follicle, such as the outer root sheath (ORS), inner root sheath (IRS), cortex and matrix (stages 5-8) (Paus et al., 1999). The crucial mesodermal component underneath the placode, the dermal papilla, is an important signalling centre for hair follicle development. Signals known to participate in hair follicle initiation, placode down growth and subsequent morphogenesis of the various parts of the follicle include Wnt, Bmp2, Bmp4 and Shh (to name a few), together with their effectors β-catenin/Lef1/Tcf, Smad proteins and patched/Gli2

[1]Max-Delbrück-Center for Molecular Medicine, Robert-Rössle-Strasse 10, 13092 Berlin, Germany. [2]Medical Biosciences, School of Life Sciences, University of Bradford, Bradford BD7 1DP, UK. [3]Department of Biochemistry, University of Lausanne, Chemin des Boveresses 155, 1066 Epalinges, Switzerland. [4]Department of Dermatology, University Hospital Schleswig Holstein, Campus Lübeck, University of Lübeck, Ratzeburger Allee 160, 23538 Lübeck, Germany.

*Author for correspondence (e-mail: rschmidt@mdc-berlin.de)

Accepted 14 December 2005

(Millar, 2002; Schmidt-Ullrich and Paus, 2005). The precise temporal sequence of most signals during hair follicle development is still unclear. Moreover, there is considerable signalling redundancy and the specific signals that direct the development of a particular hair type also remain unknown.

The distinct developmental processes regulated by NF-κB in hair follicle development are unknown. Compared with *tabby* and *downless* mice, $c^{I\kappa B\alpha\Delta N}$ mice demonstrate clear differences in phenotype severity regarding cusp formation, and number of teeth and hairs (Ohazama et al., 2004b; Schmidt-Ullrich et al., 2001). This suggests that NF-κB is not only regulated by Eda A1/EdaR in hair follicle and tooth development, but also by other additional signals. Furthermore, it was not clear to what extent NF-κB acts downstream or upstream of Eda A1/EdaR, given that the expression of several members of the TNF ligand and receptor multigene families (e.g. TNFα, LTβ, LTβ receptor, CD40, etc.) are under control of NF-κB. Therefore, the aim of the current study was to present a detailed analysis of the physiological role and regulation of NF-κB in murine primary and secondary hair follicle development.

By mating *tabby* and *downless* mice into *(Igκ)$_{3x}$cona-lacZ* (*κGal*) NF-κB reporter mice, we report here that NF-κB activity in vivo is induced downstream of Eda A1/EdaR. Importantly, NF-κB is not needed to initiate guard hair follicle placode formation. Although an attempt at hair follicle development up to pre-placode stage 0/1 takes place, no further placode down growth occurs in the absence of NF-κB. These conclusions are further supported by the resumption of NF-κB activity after treatment with recombinant Eda A1 in explants of E13.5 *tabby* × *κGal* embryos, which restores placode down growth. However, TNFα, and to a lesser extent PMA, also induce NF-κB activity and subsequent placode down growth, showing that induction of NF-κB activity is sufficient for initiating placode down-growth. In addition, we demonstrate that NF-κB is required for Eda A1/EdaR-mediated induction of Shh and cyclin D1 expression.

MATERIALS AND METHODS

Mice

Mouse strains used for this study have been described previously: $c^{I\kappa B\alpha\Delta N}$ (Schmidt-Ullrich et al., 2001), *(Igκ)$_{3x}$cona-lacZ* (=*κGal*) (Schmidt-Ullrich et al., 1996), *tabby* (Eda A1 mutant mice, kindly provided by I. Thesleff) (Gruneberg, 1971; Mikkola et al., 1999) and *downless* (EdaR mutant mice, JAX mouse strain B6C3FE-a/a-EdaR$^{dl\text{-}J}$ #000210) (Headon and Overbeek, 1999). $c^{I\kappa B\alpha\Delta N}$ and *κGal* mice were identified by PCR. Furthermore, offspring of the following matings were analysed: $c^{I\kappa B\alpha\Delta N}$ × *κGal*; *tabby* × *κGal*; *downless* × *κGal*. Mice mated into *tabby* or *downless* background were bred into homozygosity for *tabby* or *downless* mutation, respectively. Except for *tabby*, all other mouse strains are of C57Bl/6 background.

Electrophoretic mobility shift assay (EMSA) and western blotting

MEF (mouse embryonic fibroblasts) were isolated from $c^{I\kappa B\alpha\Delta N}$ mice and cultured in DMEM high glucose (GlutaMAX I, Gibco) containing 15% FCS, 1% MEM essential amino acids (Gibco), 10 mM β-mercaptoethanol and antibiotics. Total protein extracts were prepared as described by (Schmidt-Ullrich et al., 2001). Back skin epidermis of newborn $c^{I\kappa B\alpha\Delta N}$ and *downless* mice was lysed in extraction buffer [20 mM HEPES (pH 7.0), 0.15 mM EDTA, 0.15 mM EGTA, 10 mM KCl, 0.15 mM spermidine, 1% NP40, 0.4 M NaCl, 10% glycerol and protease inhibitors] by douncing. After 1 hour of shaking at 4°C, extracts were centrifuged at 86,000 ***g*** for 1 hour at 4°C and supernatants used for western blotting and EMSA analysis. EMSA was performed as described previously (Krappmann et al., 1996). Antibodies for western blotting and EMSA supershift analysis were: αIκBα (C-21, Santa Cruz), αp65 (p65(A), Santa Cruz), αp50 (D-17, Santa Cruz; and #06-886, Upstate), RelB (C-19, Santa Cruz). An anti-C-terminal β-catenin polyclonal antibody was provided by J. Huelsken.

Histology and in situ hybridization

X-Gal staining for detection of β-galactosidase activity was as described previously (Schmidt-Ullrich et al., 1996). Tissue or embryos were stained as whole-mounts, dehydrated in ethanol (30%-100%) and embedded in Technovit 7100 plastic (Heraeus Kulzer). Sections of 5-8 μm were counterstained with 0.1% pyronin G.

For immunohistochemistry, 8 μm cryosections were fixed in ice-cold acetone. Blocking was carried out in 10% goat serum. Rabbit anti-mouse antibodies against filaggrin (PRB-417P), involucrin (PRB-140C), loricrin (PRB-145P) and keratin 10 (PRB-159P) were purchased from Covance. Biotinylated goat anti-rabbit antibodies were from Jackson's Immunoresearch Laboratories. All antibody dilutions and wash steps were carried out in Tris-buffered saline (TBS, pH 7.6). For detection, the ABC-AP complex (Vector Laboratories) was added and staining for alkaline phosphatase [AP Subtsrate Kit I (red), Vector Laboratories] was carried out. Sections were counterstained with Mayer's Haematoxylin.

In situ hybridization was performed on 8 μm paraffin sections of embryonic or newborn skin. Embryos and tissue were fixed in Bouin's fixative (150 ml picric acid, 50 ml 37% formaldehyde, 10 ml glacial acetic acid), dehydrated and paraffin wax embedded. After sectioning, samples were rehydrated, post-fixed in 4% paraformaldehyde/PBS, bleached and treated with Proteinase K (Roche). Hybridization with digoxigenin (DIG)-labelled antisense and sense RNA probes was performed according to the manufacturer's protocol (Roche). The following mouse cDNAs were used: Downless (nt 302-1038, AF160502), IκBα (nt 1-1091, U36277/NM010907), Shh (nt 120-760, X76290), cyclin D1 (nt 931-2358, BC044841), Eda A1 (tabby) (nt 2309-2945, Y13438) and TROY (nt 135-591, AB040432) (Ohazama et al., 2004a). Human cDNA probes: IκBα full-length cDNA (NM020529) (Krappmann et al., 1996). After hybridization, the slides were washed as follows: (1) 60°C for 5 minutes in 5× SSC (0.75 M NaCl, 75 mM sodium citrate, pH 7.0) and 50% formamide; (2) 60°C for 10 minutes in 2× SSC and 50% formamide; (3) room temperature for 10 minutes in 2× SSC, 50% formamide, 1:1 in TES buffer (0.5 M NaCl, 10 mM Tris-HCl, pH 8.0, 1 mM EDTA); (4) 37°C for 2 minutes in TES buffer; (5) two high stringency washes at 60°C for 15 minutes in 1× SSC followed by 30 minutes in 0.2× SSC. The DIG-labelled probe was detected with an anti-DIG AP (alkaline phosphatase)-coupled Fab fragment (Roche) and subsequent BM-purple (Roche) treatment. Sections were counterstained with 0.01% PyroninG and mounted with Entellan (Merck) after dehydration. All pictures were taken with a Zeiss Axioplan 2 Imaging microscope/ Axiophot camera. Whole-mount in situ hybridization was performed as previously described (Schmidt-Ullrich et al., 2001).

Embryonic skin cultures

Skin biopsies of E13.5 embryos of *κGal* and *tabby* × *κGal* mice were harvested in PBS under a stereo microscope. The explants were then cultured for 24 hours on Millipore filters at 37°C in DMEM, supplemented with 10% FCS, 1 mM sodium pyruvate and 100 units/ml penicillin/streptomycin, using Falcon centre-well organ culture dishes and fine metal grids (Goodfellow). When indicated, recombinant purified Fc-Eda A1 or Fc-Eda A2 (Gaide and Schneider, 2003) (0.1-0.5 μg/ml) (Mustonen et al., 2004), TNFα (25 ng/ml) or PMA (200 ng/ml) were added to the culture medium. After 24 hours of culture, the skin explants were treated either for X-Gal staining or for whole-mount in situ hybridization as described above.

BrdU incorporation for cell proliferation studies

Pregnant females (E14.5 and E15.5) were injected with 100 μg BrdU (5-bromo-2-deoxyuridine, Roche)/g body weight. After 3-4 hours, embryos were removed, fixed in Bouin's and embedded in paraffin wax as described above. Sections (5 μm) were cut. Sections were dewaxed, rehydrated and then bleached with 0.3% H_2O_2 in methanol. DNA fragmentation was preformed in 1 M HCl at 37°C for 5 minutes. After protein digestion with 50 μg Proteinase K (Roche) for 5 minutes at 37°C, sections were refixed in 3.7% formaldehyde for 5 minutes at room temperature. For BrdU detection, the Vector M.O.M. Immunodetection Kit for peroxidase (Vector Laboratories, #PK-2200) was used, together with a mouse monoclonal anti-

BrdU antibody (Sigma; Clone BU33). The POD substrate reaction was carried out with DAB (Sigma). Sections were counterstained with Haematoxylin.

High resolution light microscopy (HRLM) and transmission electron microscopy (TEM)

E14.5 and E15.5 embryos were fixed for 3 hours at 4°C in Karnovsky's fixative (sodium cacodylate buffer, 4% paraformaldehyde, 25% glutaraldehyde, $CaCl_2$, pH 7.2-7.4) (Karnovsky, 1965), and then washed with 0.1 M cacodylate buffer. Embryos were then post-fixed in 2% osmium tetroxide, uranyl acetate and embedded in araldite resin as previously described (Tobin et al., 1990; Tobin et al., 1991). Semi-thin HRLM sections were stained with metachromic stain, toluidine blue/borax, examined under light microscope (oil-immersion) and photographed (Leitz, Germany). Ultra-thin TEM sections were stained with uranyl acetate and lead citrate, and examined and photographed using a Jeol 100CX electron microscope (Jeol, Tokyo, Japan).

RESULTS

$c^{I\kappa B\alpha\Delta N}$ mice show reduced NF-κB p50-p65 activity in skin, but normal epidermal keratinocyte differentiation

We have previously shown that $c^{I\kappa B\alpha\Delta N}$ mice do not develop guard and zigzag pelage hair follicles. Analysis of IκBαΔN expression, under the control of the β-catenin locus, in the skin of P0 $c^{I\kappa B\alpha\Delta N}$ knock-in mice displayed readily detectable amounts of IκBαΔN protein (Fig. 1A). This was expected because β-catenin mRNA and protein is highly expressed in hair follicles and interfollicular epidermis at any developmental stage, and, thus, guarantees expression of the super-repressor IκBαΔN at these sites (data not shown) (Huelsken et al., 2001). Endogenous IκBα and β-catenin protein amounts remained unchanged (Fig. 1A). The EMSA confirmed equally reduced binding of p50-p65 complexes for $c^{I\kappa B\alpha\Delta N}$ and *downless* (EdaR-mutant) mice (Fig. 1B). The faint p50-p65 DNA binding activity in wild-type skin is expected, considering the few cells with active NF-κB in hair follicles, when compared with interfollicular epidermal keratinocytes without any detectable NF-κB activity (see below). The residual NF-κB DNA-binding complexes in $c^{I\kappa B\alpha\Delta N}$ and *downless* mice may account for constitutive activity, independent of IκBα degradation and of Eda A1/EdaR signalling in the skin. We detected only p50-p65 (NF-κB) complexes, apart from very prominent p50 homodimer binding in the epidermis. We can conclude that overall heterodimeric NF-κB activity is reduced in $c^{I\kappa B\alpha\Delta N}$ and *downless* mice.

In NF-κB reporter mice (*κGal*), we had already observed that there was no NF-κB activity in the interfollicular epidermis before and after birth (Schmidt-Ullrich et al., 2001; Schmidt-Ullrich et al., 1996). $c^{I\kappa B\alpha\Delta N}$ mice manifest neither any hyperproliferation of the skin nor any inflammatory processes, seen in $Ikka^{-/-}$, $Relb^{-/-}$ or $K14\text{-}Cre/Ikkb^{Fl/Fl}$ mice (Barton et al., 2000; Hu et al., 2001; Pasparakis et al., 2002). Keratinocyte differentiation was examined and was found to proceed normally in $c^{I\kappa B\alpha\Delta N}$ mice (Fig. 1C). Typical markers for terminal keratinocyte differentiation (loricrin, involucrin, filaggrin and spinous layer marker keratin 10) were expressed in patterns indistinguishable from wild type (Fig. 1C). Thus, NF-κB activity is not needed for epidermal keratinocyte differentiation. This is in agreement with IKKα-deficient mice, where terminal differentiation was blocked independently of NF-κB (Hu et al., 2001).

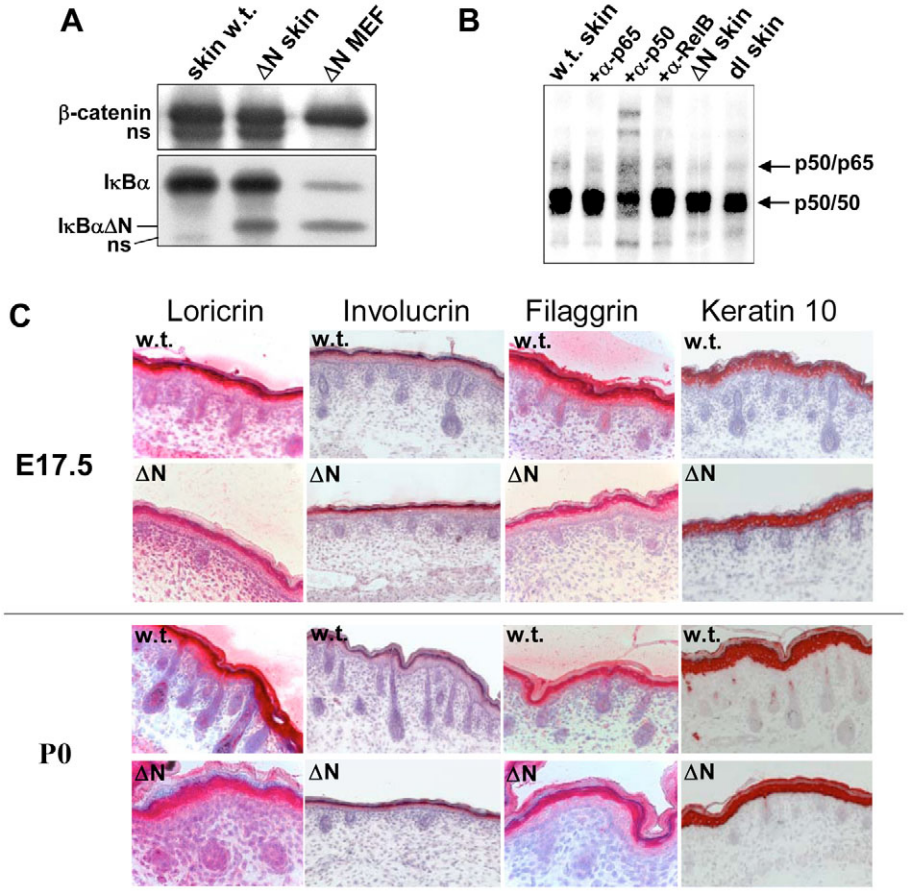

Fig. 1. Reduced NF-κB activity in skin of $c^{I\kappa B\alpha\Delta N}$ and *downless* mice, but normal perinatal epidermal keratinocyte differentiation in $c^{I\kappa B\alpha\Delta N}$ mice. (**A**) Total protein extracts of newborn wild-type and $c^{I\kappa B\alpha\Delta N}$ (ΔN) skin were analysed for IκBαΔN expression in a western blot using an anti-IκBα antibody (lower panel). Mouse embryonic fibroblasts isolated from $c^{I\kappa B\alpha\Delta N}$ mice were used as a positive control (ΔN MEF, right lane). β-Catenin protein levels remained unchanged in all extracts (upper panel). ns, non-specific. (**B**) EMSA of total skin extracts of newborn wild-type, $c^{I\kappa B\alpha\Delta N}$ (ΔN) and *downless* (dl) skin. Extracts were treated with specific antibodies against NF-κB p65, p50 and RelB as indicated, which inhibited (α-p65) or upshifted (α-p50) the DNA-binding complex. No effect was seen with RelB. Strong p50 homodimer binding is present in skin extracts. (**C**) Sagittal cryosections of E17.5 and P0 wild-type and $c^{I\kappa B\alpha\Delta N}$ (ΔN) embryos were incubated with antibodies to different epidermal differentiation markers (AP substrate, in red), as indicated above (loricrin, involucrin, filaggrin, keratin 10). Counterstaining was carried out with Mayer's haemalaun (blue).

In developing pelage hair follicles NF-κB activity is first observed in pre-placode stage at E14.5

Because placode formation in $c^{I\kappa B\alpha\Delta N}$ mice was interrupted at a very early time point of development, we analysed NF-κB activity at all stages of normal pelage hair formation (Fig. 2). Whole-mount and Technovit plastic sections of E10-P0 embryos of *κGal* mice revealed that first NF-κB activity in the epidermis was observed at E14.5 in an placode-initiating (pre-placode) stage, here defined as stage 0/1, in guard hair placodes (Fig. 2B). At stage 1 and 2, the activity became restricted to the proximal part of the placode, which grows downwards to invaginate the mesenchyme (Fig. 2B). At later stages of guard hair follicle morphogenesis (>E17) and in all adult follicles, NF-κB activity is detected in the matrix, cortex, inner root sheath and the sebaceous gland (Fig. 2B) (Schmidt-Ullrich et al., 2001). NF-κB activity was also present in a similar expression pattern in all secondary hair follicle placodes, including awl hairs, although awl hairs develop in $c^{I\kappa B\alpha\Delta N}$ mice. However, in $c^{I\kappa B\alpha\Delta N}$ mice, awl hairs do have a slightly different shape, resulting in an awl/tylotrich intermediate, as was previously also described for *tabby* mice (Falconer, 1952; Schmidt-Ullrich et al., 2001). The typical ultrastructure could, thus, be regulated by NF-κB. At earlier embryonic days (E13.5 or before), NF-κB was seen in endothelial cells of dermal blood vessels (Fig. 2A,B). At P0 and later, occasional X-Gal staining is also seen in dermal fibroblasts (data not shown). No NF-κB activity is observed in the interfollicular epidermis or dermal papilla at any time point (Fig. 2B). In conclusion, during hair follicle development NF-κB activity is mainly observed in the proximal part of pelage hair placodes, indicating a role in proliferation and down growth of hair placodes.

Formation of guard hair placodes is attempted in $c^{I\kappa B\alpha\Delta N}$ and *downless* mice, but EdaR and NF-κB are needed for subsequent keratinocyte proliferation and placode down-growth

Detailed morphological analysis of embryonic skin (E14.5, E15.5) of *downless* and $c^{I\kappa B\alpha\Delta N}$ mice using high resolution light microscopy (HRLM) disclosed that initiation of primary guard hair placode formation took place in these mice (Fig. 3A, upper panel). Characteristic early signs of placode formation were observed, such as localized accumulation of ectodermal keratinocytes, adopting an upright position (Fig. 3A, lower panel, pre-placode stage 0/1) (see Paus et al., 1999; Schmidt-Ullrich and Paus, 2005). Yet, any further developmental process was arrested in these mice at pre-placode stage 0/1 (Fig. 3A).

To study further the role of NF-κB in proliferation of placode keratinocytes, expression of G1 phase cyclin D1, a target gene of NF-κB in several cell types (Hinz et al., 1999), and bromodeoxyuridine (BrdU) incorporation (as an S-phase marker) were analysed. Surprisingly, cyclin D1 was not upregulated until hair placode developmental stage 1/2 and was highly expressed at germ and peg stage 2-3 at E15.5 (Fig. 3B). At developmental stage 1, only very weak cyclin D1 expression was detected (Fig. 3B). Thus, the late cyclin D1 upregulation does not coincide with the

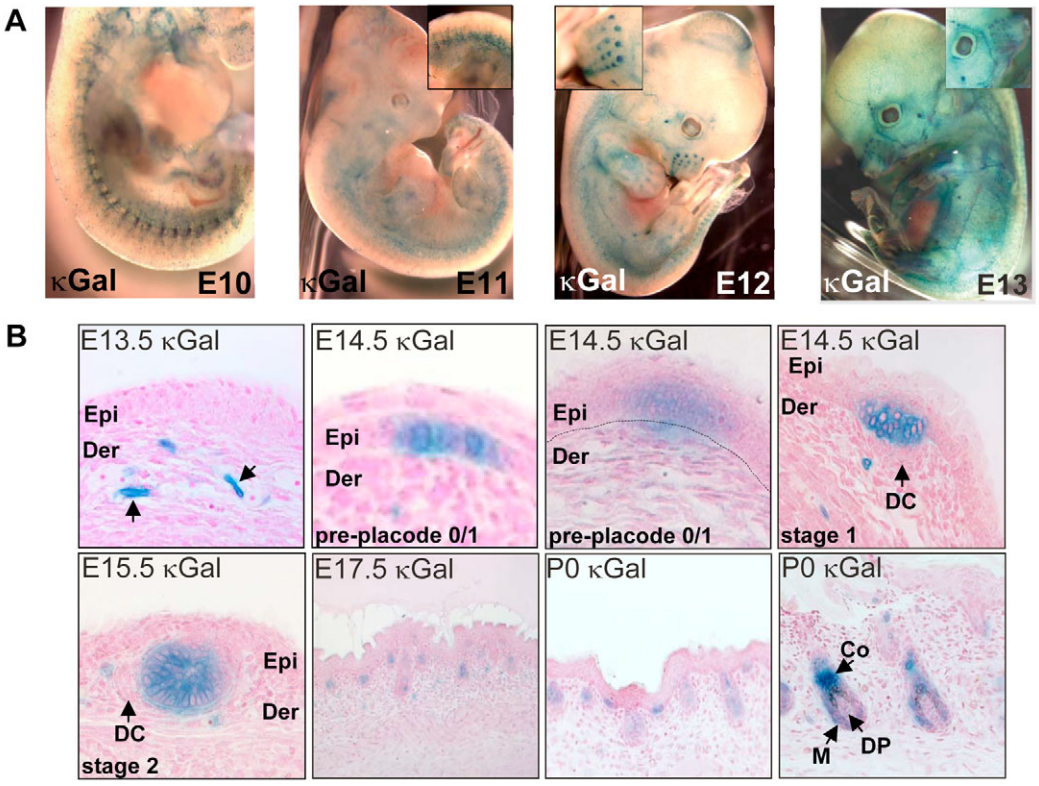

Fig. 2. NF-κB activity during embryonic vibrissae and hair follicle development analysed in NF-κB-driven β-Gal reporter mice. (**A**) Whole-mount X-Gal staining of E10-13 *(Igκ)$_{3x}$cona-lacZ* (*κGal*) embryos. At E10-11, NF-κB activity is observed only in somites and endothelial cells of blood vessels. From E12 onwards, activity is seen in vibrissae follicles and the rim of the eyelids (see also insets E12 and E13). (**B**) Sagittal sections of X-Gal stained embryonic and newborn skin were performed to analyse the most important stages of murine pelage hair follicle development. At E13.5, arrows indicate endothelial cells of blood vessels. M, matrix; Co, pre-cortex; DC, dermal condensate; DP, dermal papilla. Broken line indicates the boundary between epidermis (Epi) and dermis (Der).

start of Eda A1/EdaR/NF-κB signalling (stage 0/1, E14). However, Shh upregulation coincides and co-localizes with cyclin D1 expression at stages 2-3 (Fig. 6B, Fig. 3B). No cyclin D1 expression was seen in developing guard hair follicles of $c^{I\kappa B\alpha\Delta N}$ mice. However, normal cyclin D1 expression was observed in vibrissae and secondary awl hairs of $c^{I\kappa B\alpha\Delta N}$ mice (Fig. 3B; data not shown).

BrdU incorporation revealed that proliferative cells were readily detected from stage 0/1 on in wild-type guard hair placodes, while in areas of attempted hair follicle formation in $c^{I\kappa B\alpha\Delta N}$ mice proliferative cells were missing (Fig. 3C). In wild-type embryos, the proliferative cells were seen in the proximal part of placodes where NF-κB activity was observed in *κGal* mice (see Fig. 2). The above results strongly suggest a role of NF-κB in proliferation and down growth of guard hair placodes.

Lack of NF-κB activity leads to loss of structural organization of the developing epidermis

HRLM and TEM analysis of E14.5 (Fig. 3A, Fig. 4A) and E15.5 (Fig. 3A, Fig. 4B) *downless* and $c^{I\kappa B\alpha\Delta N}$ mice showed a severe loss of structural organization in the epidermis at sites of placode formation when compared with wild-type embryos at the same stage. These degenerative processes may be the result of a lack of further placode down growth. There was a pronounced reduction in the number and size of desmosomal junctions, increased vacuolization of keratinocytes and increased apoptosis in the epidermis and the underlying dermis at sites of placode formation at E14.5 in $c^{I\kappa B\alpha\Delta N}$ and *downless* mice (Fig. 4A, middle and lower panels). In cell lines and some tissues, the lack of NF-κB activity, especially in the presence of TNF signalling, is known to cause apoptosis (Aggarwal, 2003). However, in $c^{I\kappa B\alpha\Delta N}$ and *downless*

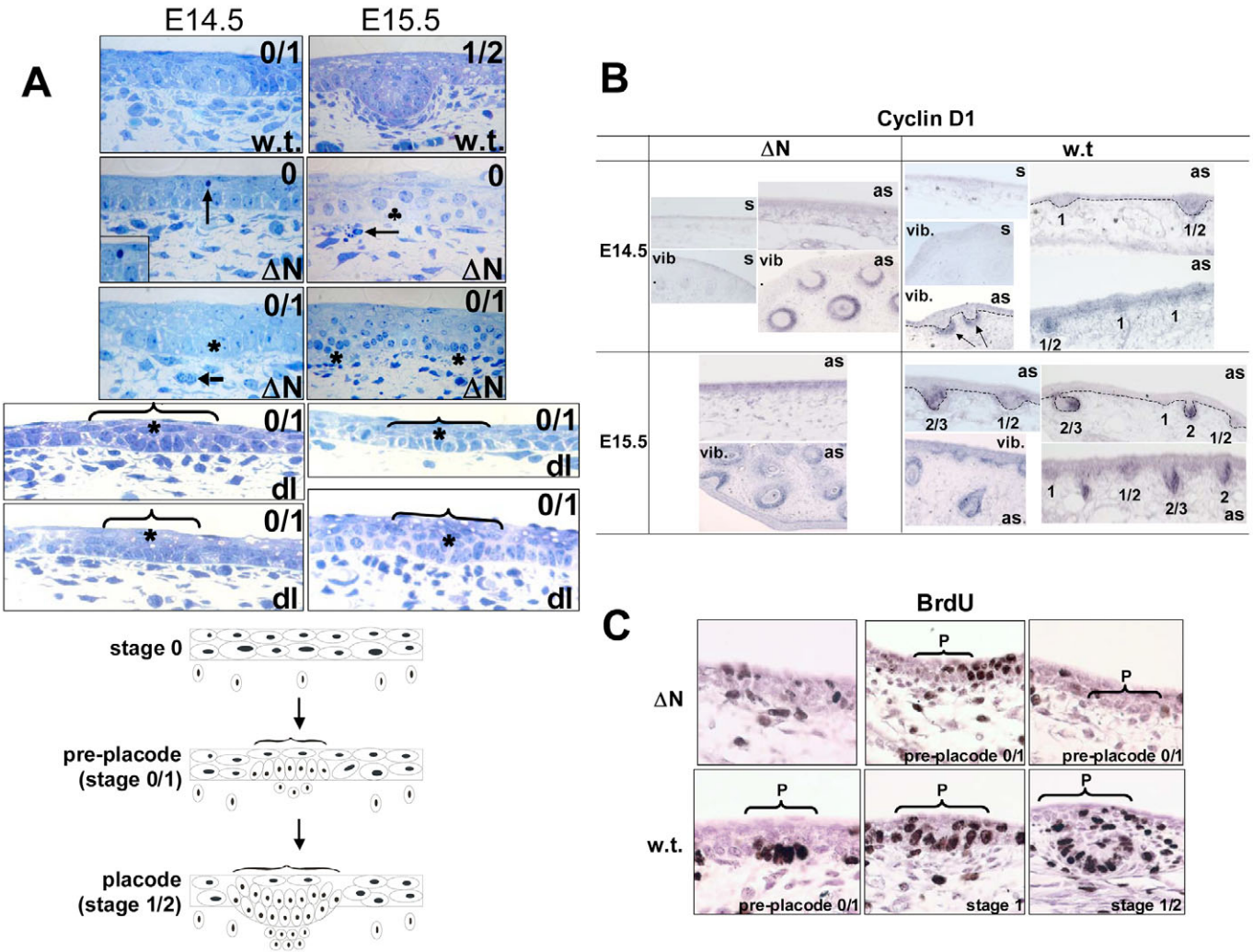

Fig. 3. NF-κB regulates down growth, but not initiation of primary guard hair follicle placodes. (**A**) Upper panel: high-resolution light microscopy of sagittal sections of wild-type, $c^{I\kappa B\alpha\Delta N}$ (ΔN) and *downless* (*dl*) mice. Embryos were analysed at E14.5 and E15.5. Developmental stage of placodes is indicated in each panel (0-1/2). Lower panel shows a schematic presentation of the first typical morphological changes observed during hair follicle induction (see also Paus et al., 1999). Brackets indicate placode borders, long arrows indicate apoptosis and short arrow indicate mitosis. Asterisks indicate attempted hair follicle formation; the club indicates loss of structural organisation. (**B**) In situ hybridization of wild-type and $c^{I\kappa B\alpha\Delta N}$ (ΔN) mice at E14.5 and E15.5 using a cyclin D1 sense and antisense probe. Vibrissae follicles also show cyclinD1 expression in dermal condensate (wild type E14.5). s, sense probe; as, anti-sense probe; vib., vibrissae. Stages of hair follicle development are indicated beneath placodes in wild-type sections. Broken lines indicate the boundary between epidermis and dermis. (**C**) Analysis of cell proliferation in the epidermis of E14.5 and E15.5 wild-type and IκBαΔN (ΔN) embryos. BrdU incorporation into the DNA was detected with an anti-BrdU antibody and subsequent peroxidase reaction (brown nuclei). There are also a few nuclei stained in the interfollicular epidermis and dermis of wild-type and ΔN embryos. Developmental stages are indicated in each panel. P, placode. Brackets indicate placode borders.

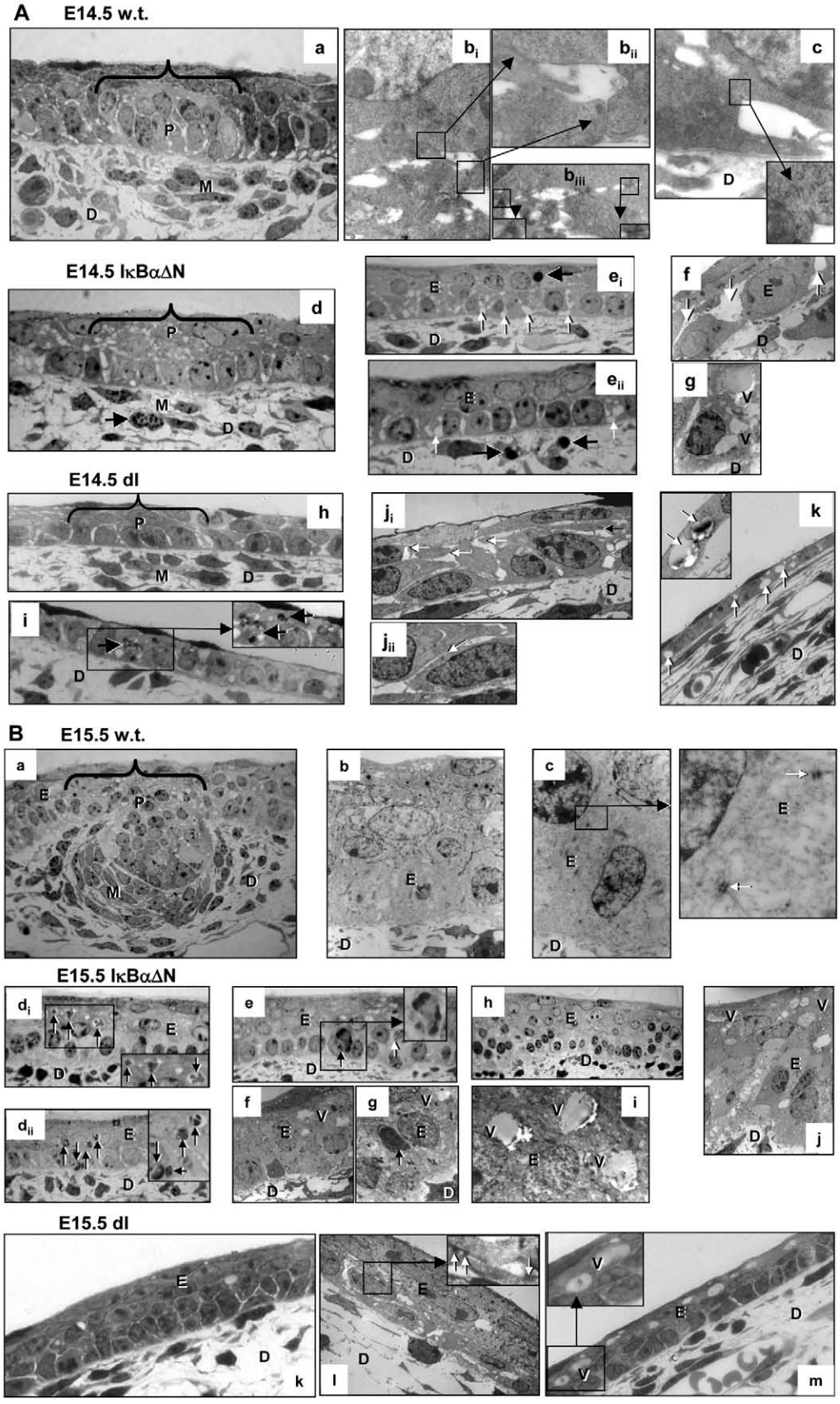

Fig. 4. Loss of epidermal structure resulting from reduced cell-cell contacts, significant apoptosis and vacuolization of keratinocytes during early guard hair follicle development in $c^{I\kappa B\alpha\Delta N}$ (IκBΔN) and *downless* (dl) compared with wild-type mice. High-resolution light microscopy and electron microscopy images of embryos at E14.5 (A) and E15.5 (B). (**A**, a) Hair follicle placode stage 0/1 in wild-type embryo. Focal reorganization of basal keratinocytes with clustering of mesenchymal cells. (b,c) Cell-cell contact maintained by intercellular junctions, e.g. desmosomes. No vacuoles. (d) Hair follicle placode stage 0/1 in $c^{I\kappa B\alpha\Delta N}$ embryo. Focal reorganization of basal keratinocytes, especially cell parallelization, and an attempt at clustering of mesenchymal cells with mitosis (arrow). (e) Apoptotic cells in epidermis and mesenchyme (black arrows). (e-g) Lack of cohesion of basal cells (white arrows) with associated vacuoles containing lipid-like material. (h,i) Hair follicle placode stage 0/1 in *downless* embryo. (h) Focal reorganization of basal keratinocytes via cell parallelization and clustering of mesodermal cells. (i) Increased apoptosis in epidermis (black arrows). (j) Lack of cohesion of basal cells (white arrows). (k) Vacuoles containing lipid-like material in epidermis (white arrows). (**B**, a) Hair follicle placode stage 2 in wild-type embryo. Development of hair peg and significant clustering of mesenchymal cells forming the dermal condensate. (b,c) Epidermal cell-cell contacts maintained by intercellular junctions, including desmosomes. No vacuoles. (d) Hair follicle placode stage 0 in $c^{I\kappa B\alpha\Delta N}$ embryo. No placode development detectable. (d,e,h) Significant apoptosis (black arrows). Cell-cell contacts are maintained by intercellular junctions, including desmosomes, and intercellular spaces are less than at E14.5. Vacuoles containing lipid-like material present. (h,j) Cellular disorganization with poor stratification. (k) Hair follicle placode stage 0 in *downless* embryo. (k,i,l) No placode development detectable. Cell-cell contacts are maintained as in $c^{I\kappa B\alpha\Delta N}$ and there are fewer intercellular spaces than at E14.5. (m) Vacuoles containing lipid-like material present. P, basal keratinocytes, clustering in hair placodes; M, mesenchymal cells, clustering to form dermal condensate; V, vacuoles; D, dermis; E, epidermis.

mice, apoptosis was mostly observed in the suprabasal layer of the epidermis and also in the underlying dermal condensate, where NF-κB is normally not activated. It may, therefore, be related to the general loss of structure and attempt of reorganization in the absence of placode formation. The vacuoles observed in the degenerating keratinocytes contained lipid-like material (see Fig. 4A). The reason for the vacuolization remains unknown. At E15.5, apoptosis in the suprabasal layer of the epidermis remained or even increased, but intercellular contacts such as desmosomes were being rebuilt, leading to less intercellular spaces than observed at E14.5 (Fig. 4B). This indicates that, at E15.5, the epidermis begins to regain its normal organization.

NF-κB in vivo is downstream of Eda A1 and EdaR

Previous overexpression studies in transformed cell lines have shown that NF-κB can be activated by Eda A1 and EdaR via the IKK pathway (Kumar et al., 2001). It was important to investigate whether in vivo NF-κB acts downstream of Eda A1/EdaR. For this purpose, *tabby* (mutant Eda A1), *downless* (mutant EdaR) and, as a control, $c^{I\kappa B\alpha\Delta N}$ mice were mated into *κGal* reporter mice (Fig. 5A). Embryos from these matings did not reveal any NF-κB activity in guard hair placodes at E14 and E15 (Fig. 5A). As expected, in $c^{I\kappa B\alpha\Delta N}$ × *κGal* embryos, NF-κB activity was blocked, whereas in *tabby* or *downless* × *κGal* embryos activity was still present in endothelial cells of the blood vessels and other sites independent of Eda A1/EdaR signalling (Fig. 5A, and data not shown).

In newborn mice of the same matings, NF-κB activity was also strongly reduced (*tabby* and *downless* × *κGal*) or absent ($c^{I\kappa B\alpha\Delta N}$ × *κGal*) in all secondary hair follicles (Fig. 5B, right panel), which did show NF-κB activity in wild-type *κGal* mice (Fig. 2B). Therefore, NF-κB is activated downstream of Eda A1/EdaR in all primary and secondary follicles, including awls, which demonstrates that development of awl hairs is mainly independent of NF-κB activity. However, the residual NF-κB activity in many secondary hair placodes of *tabby* or *downless* × *κGal* at P0 (Fig. 5B) supports our finding of a more severe phenotype in $c^{I\kappa B\alpha\Delta N}$ mice with regard to zigzag hair and molar tooth development, compared with *tabby* mice (see Fig. 7) (Cui et al., 2003; Ohazama et al., 2004b). This suggests that in these ectodermal organs NF-κB is regulated by additional signals.

The observed activity of NF-κB in guard hair placodes at E14.5 coincided with localized EdaR expression at this site. By contrast, EdaR was still uniformly expressed in the entire epidermis in wild-type and in $c^{I\kappa B\alpha\Delta N}$ mice at E13.5 (Fig. 5C), supporting previous observations (Headon and Overbeek, 1999). Some localized EdaR expression is also observed in $c^{I\kappa B\alpha\Delta N}$ mice at E14-E14.5, while at E15.5 EdaR expression was absent (Fig. 5C). The mechanism which prevents EdaR expression in interfollicular epidermis, instead restricting it to placodes around E14, currently remains unknown. However, this event can still occur in $c^{I\kappa B\alpha\Delta N}$ mice. The complete absence of placodal EdaR expression at E15.5 can be interpreted in two ways. First, that NF-κB is responsible for further EdaR upregulation. However, this possibility is contrary to the observation that EdaR expression was normal in awl hairs of $c^{I\kappa B\alpha\Delta N}$ mice at E17.5 and P0 (Fig. 5C). Second, placodal keratinocytes may rapidly reorient themselves to epidermal keratinocytes in the absence of further specific placode growth signals (see Fig. 4).

Note that in wild-type embryos, EdaR expression is located in the downgrowing, proximal part of the placode, identical to NF-κB activity in *κGal* reporter mice (see Fig. 5C). No differences of EdaR expression between wild-type and $c^{I\kappa B\alpha\Delta N}$ mice were observed in secondary awl hairs at E17.5 and P0, and in vibrissae follicles at any time point (Fig. 5C). Ubiquitous ectodermal Eda A1 expression levels in *downless* and $c^{I\kappa B\alpha\Delta N}$ mice were also indistinguishable from those in wild-type mice at all time points, demonstrating that Eda A1 expression does not require NF-κB (Fig. 5C). In wild-type mice, Eda A1 expression was typically absent from the early placodes, while Eda A1 was observed later in hair germs and peg stages, and in the hair follicle matrix and pre-cortex (Fig. 5C, P0). The Eda A1 mRNA probe used for this experiment recognizes all Eda A1 mRNA isoforms.

NF-κB activity in hair placodes was further verified by using a murine anti-sense probe of IκBα, which is a known NF-κB target gene in cells with activated NF-κB p50/p65 complexes (Fig. 5C) (Le Bail et al., 1993). As expected, in wild-type embryos, IκBα mRNA expression was strongly upregulated in the proximal part of guard hair placodes at E14.5 and E15.5 (Fig. 5C). In $c^{I\kappa B\alpha\Delta N}$ and *downless* embryos, no IκBα mRNA expression was detected in the epidermis, but upregulation was detected in vibrissae (Fig. 5C, E14.5 and E15.5). The lack of IκBαΔN RNA detection in $c^{I\kappa B\alpha\Delta N}$ mice was presumably due to low affinity of the mouse IκBα mRNA probe for the human IκBαΔN RNA. However, a human IκBα mRNA probe revealed strong IκBαΔN expression throughout the epidermis and in secondary hair follicles of $c^{I\kappa B\alpha\Delta N}$ mice, while in wild-type mice, there was only very weak staining because of low cross-reaction with endogenous mouse IκBα (Fig. 5C). At P0, both wild-type and $c^{I\kappa B\alpha\Delta N}$ mice presented IκBα mRNA upregulation in all secondary hair and late-stage guard follicles, and in the basal layer of the interfollicular epidermis (Fig. 5C, mouse IκBα). The upregulation of IκBα mRNA in the basal layer, and in vibrissae and awl hairs of $c^{I\kappa B\alpha\Delta N}$ mice is either independent of NF-κB activity, or the NF-κB activity in these cells is so low that it is not detectable in the κGal mice. Thus, we have formally proven that in vivo NF-κB acts downstream of Eda A1/EdaR. The integration of NF-κB into the EdaA1/EdaR signalling pathway with all its components is depicted in Fig. 8.

Re-induction of NF-κB activity is sufficient to re-establish placode down-growth in *tabby* skin explants

To investigate whether activation of NF-κB can restore placode down growth, skin explants of *tabby* × *κGal* embryos at E13.5 were treated with recombinant Fc-Eda A1, Fc-Eda A2, TNFα or PMA for 24 hours (Fig. 6A). Eda A1 has previously been shown to be able to recover placode induction in *tabby* mice (Mustonen et al., 2004). Eda A2, a ligand of XEDAR (X linked ectodermal dysplasia receptor), was used as a negative control, as it did not induce NF-κB activity in hair follicles and cannot restore hair growth in *tabby* mice (Gaide and Schneider, 2003; Mustonen et al., 2003).

At E13.5 + 1 day (=E14.5), X-Gal staining showed that NF-κB activity in hair placodes was only re-established in Eda A1- but not in Eda A2-treated explants (Fig. 6A, upper panels). The Fc-Eda A1 also induced NF-κB in surrounding keratinocytes, because at E13.5 EdaR is still expressed uniformly in the epidermis, before it becomes restricted to placodes at E13.5 + 1 day (Fig. 6A, upper panels). Endogenous Eda A1 is obviously not in its active form at E13.5 and, thus, is not yet able to interact with EdaR to activate NF-κB. The recombinant Fc-Eda A1, however, simulates the active form of Eda A1.

TNFα stimulated NF-κB ubiquitously, including the dermis and some blood vessels, and, thus, placodes were not clearly distinguishable anymore in *tabby* × *κGal* explants. However, an antisense probe of sonic hedgehog (Shh), which is an important placode marker (St-Jacques et al., 1998) acting downstream of Eda

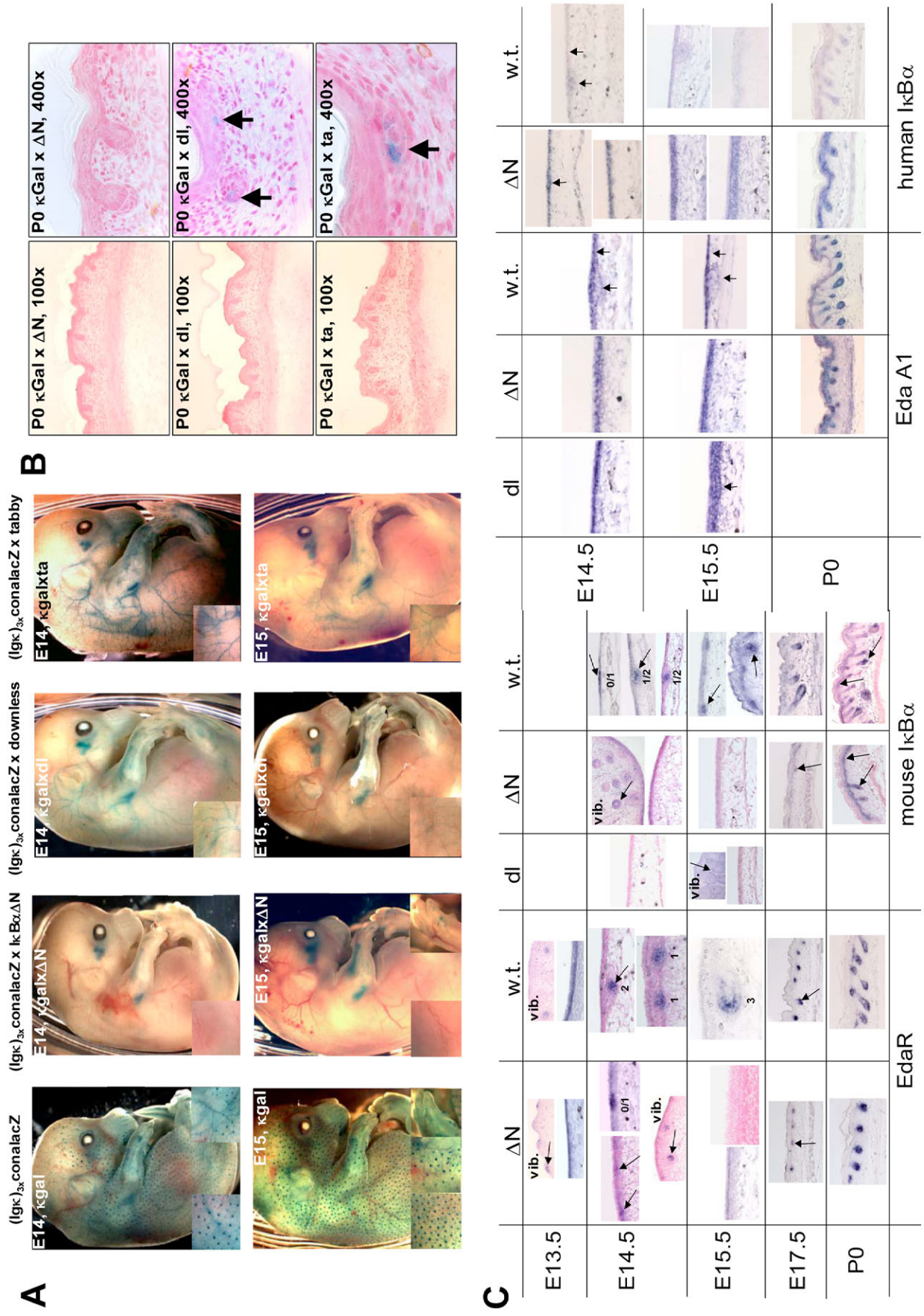

Fig. 5. See next page for legend.

Fig. 5. In vivo NF-κB activity is downstream of Eda A1/EdaR. (**A**) *κGal* NF-κB reporter mice ($(Ig\kappa)_{3x}$conalacZ, κgal) were mated into $c^{I\kappa B\alpha\Delta N}$ (IκBαΔN, ΔN), *downless* (dl, mutant EdaR) or *tabby* (ta, mutant Eda A1) mice, and analysed by X-Gal test at the time point of guard hair placode initiation. Upper panels, E14; lower panels, E15. *κGal* x $c^{I\kappa B\alpha\Delta N}$ mice only revealed some background staining close to the eye and elbow. In *κGal* × *downless* and × *tabby* embryos, X-Gal staining was absent in the placodes, but present in blood vessels (see lower left insets). (**B**) Technovit sections of X-Gal stained P0 skin of the same matings as indicated in the top left. For X-Gal staining in newborn wild-type *κGal* skin, see Fig. 2B. (**C**) In situ hybridization of sagittal paraffin sections of wild-type, $c^{I\kappa B\alpha\Delta N}$ and *downless* (*dl*) embryos at indicated time points, using EdaR, mouse IκBα, Eda A1 and human IκBα antisense probes. vib., vibrissae. Arrows indicate follicle placodes and (in Eda A1) interfollicular epidermis. 0/1–3, developmental stages of hair placode.

A1/EdaR/NF-κB (Fig. 6B), revealed that both EDA A1 and TNFα strongly reactivated Shh expression and, thus, placode formation (Fig. 6A, lower panel). It is of significance, that TNFα does not interact with EdaR (data not shown; P.S., unpublished). Thus, TNFα can activate NF-κB independently of EdaR in the epidermis. PMA only faintly restored Shh expression and placode formation, indicating that keratinocytes do not respond strongly to phorbol esters (Fig. 6A). These results not only provide additional proof that in vivo NF-κB is downstream of Eda A1, but demonstrate that reactivation of NF-κB is sufficient to continue guard hair placode development.

Shh mRNA expression was absent in primary guard hair placodes of $c^{I\kappa B\alpha\Delta N}$ and *downless* embryos at E14.5 and E15.5, and did not appear until E17, when awl hairs develop (Fig. 6B and data not shown). In *tabby* mice, Shh expression showed the same temporal expression pattern (Laurikkala et al., 2002). In guard hairs of wild-type embryos Shh was first detected at developmental stage 1-2 (Fig. 6B, E14.5 wild type), and became strongly upregulated at germ-peg stage (stage 2-3; Fig. 6B, E15.5 wild type), which is the stage where hair development is arrested in $Shh^{-/-}$ mice (Mill et al., 2003; St-Jacques et al., 1998) (for a review, see Schmidt-Ullrich and Paus, 2005). In conclusion, in guard hairs Shh expression depends directly or indirectly on NF-κB activity and, thus, is induced downstream of Eda A1/EdaR/NF-κB signalling. In awl hairs, Shh expression is independent of NF-κB.

Total number of secondary hairs is reduced in $c^{I\kappa B\alpha\Delta N}$ mice

We have reported previously that $c^{I\kappa B\alpha\Delta N}$ mice also lack fine zigzag underhairs and, thus, adult animals have greatly decreased numbers of hair follicles overall (Schmidt-Ullrich et al., 2001). At E17.5, hair numbers were reduced because of absence of guard hairs and at P0 they only presented with about 50% of wild-type hair numbers (Fig. 7A, upper and lower panels). The analysis of the different stages of HF development at E17.5 and P0 supported the fact that only one hair type from the second wave (awls) develops in $c^{I\kappa B\alpha\Delta N}$ mice (Fig. 7B). However, there are currently no mechanisms to differentiate correctly between awl, auchene or zigzag placodes, except for the initiation time points of the second (E16, awl/auchene) and third (E18/P0, zigzag) wave (Philpott and Paus, 1998; Schmidt-Ullrich and Paus, 2005) (see also Fig. 8). Thus, most stage 1 placodes at P0 are likely to give rise to zigzag hair follicles, which do not develop until around birth, i.e. during the third wave of hair follicle development (Schmidt-Ullrich and Paus, 2005; Vielkind and Hardy, 1996). $c^{I\kappa B\alpha\Delta N}$ mice mainly presented germ stage placodes at E17.5, and germ and peg stage placodes at P0, while in wild-type mice, several different stages were present in an almost equal distribution (Fig. 7B). At P0, in $c^{I\kappa B\alpha\Delta N}$ mice, only very few stage 1 placodes were detected compared with wild-type mice (Fig. 7B). This is an indication that in $c^{I\kappa B\alpha\Delta N}$ mice, zigzag follicles may stop developing at a very early stage, similar to guard hair follicles.

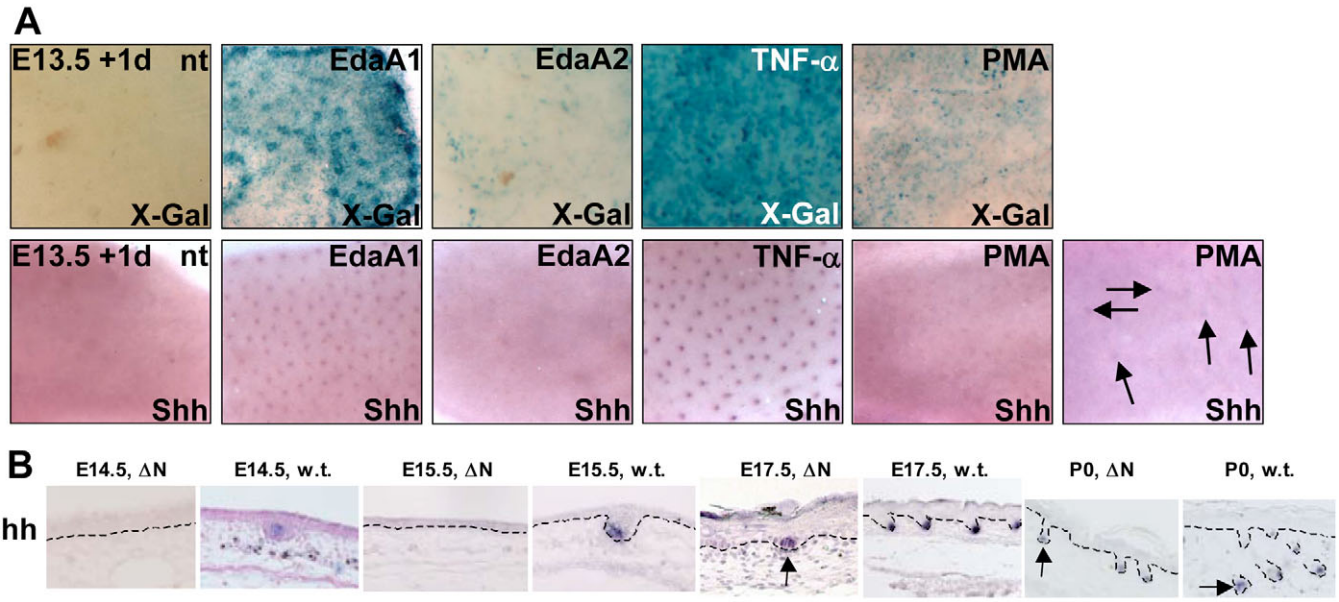

Fig. 6. NF-κB is essential and sufficient to induce placode down growth and Shh expression. (**A**) Embryonic skin explants of E13.5 *κGal* × *tabby* matings were incubated for 24 hours with recombinant Fc-Eda A1, Fc-Eda A2, TNFα or PMA or left untreated (nt). Upper row, X-Gal staining of skin explants. Lower row, whole-mount in situ hybridization of skins using an Shh antisense probe. Placode down growth was induced more or less strongly by any stimulator of NF-κB activity, except for Eda A2. (**B**) In situ hybridization of sagittal embryonic wild-type and $c^{I\kappa B\alpha\Delta N}$ (ΔN) skin sections at indicated time points (E14.5-P0) using a Shh antisense probe. Broken lines indicate the boundary between epidermis and dermis. Arrows indicate Shh-positive follicles.

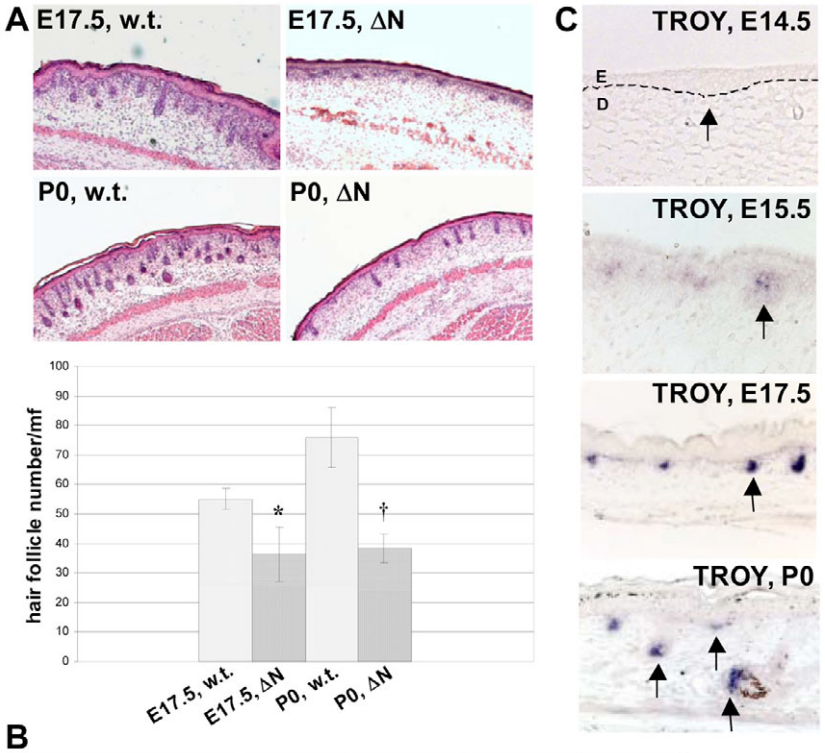

B

	E17.5, w.t.	E17.5, ΔN	P0, w.t.	P0, ΔN
stage 1, placode	32%	18%	15%	6%
stage 2, germ	28%	82%	30%	57%
stage 3, peg	26%	0%	10%	35%
stage 4, peg	14%	0%	20%	2%
stage > 5, bulbous peg	0%	0%	25%	0%

Fig. 7. NF-κB is needed for secondary zigzag hair development, where it may also be regulated by TROY. (**A**) Upper panel: cryosections of E17.5 and P0 wild-type and $c^{I\kappa B\alpha\Delta N}$ (ΔN) mice, stained with Haematoxylin/Eosin. Lower panel: hair follicle numbers of E17.5 embryos [wild type, $c^{I\kappa B\alpha\Delta N}$ (ΔN); *n*=3 each] and newborn (P0; *n*=9 $c^{I\kappa B\alpha\Delta N}$, *n*=6 wild type) were counted per microscopic field (mf). Mean values were calculated and presented in bar graphs, including standard deviations. *P* values show a significant difference: **P*<0.0158 versus wild type. for E17.5, and $^{\dagger}P$<0.0001 versus wild type for P0. At P0, the mean value reveals 50% less hairs in $c^{I\kappa B\alpha\Delta N}$ mice compared with wild type: 38/mf in $c^{I\kappa B\alpha\Delta N}$ versus 75/mf in wild type. (**B**) The different developmental stages of hair follicle development (stage 1, placode – early bulbous peg stage 5, indicated to the left of the table) in wild type and $c^{I\kappa B\alpha\Delta N}$ (ΔN) mice at E17.5 and P0 are presented in percentage (%) of total number of hairs. (**C**) In situ hybridization of sagittal skin sections of E14.5, E15.5, E17.5 and P0 embryos using a TROY antisense probe. Broken line indicates the boundary between epidermis (E) and dermis (D). Arrows indicate placodes and (at P0) the matrix of a guard hair follicle.

The more severe phenotype of $c^{I\kappa B\alpha\Delta N}$ mice compared with *tabby* and *downless* mice, and our finding that there is still some residual NF-κB activity found in secondary hair follicles of *tabby* and *downless* × *κGal* mice, implies that factors other than Eda A1/EdaR must regulate NF-κB activity in zigzag hairs. These may include two recently discovered members of the TNF family, e.g. XEDAR and its ligand Eda A2, and the orphan receptor TAJ/TROY (Tnfrsf19 – Mouse Genome Informatics), the ligand of which remains unknown (Kojima et al., 2000; Yan et al., 2000). Both proteins are expressed in hair follicles and in teeth, and are known to activate NF-κB in vitro (Kojima et al., 2000; Ohazama et al., 2004a; Yan et al., 2000). Although studies with XEDAR-deficient mice revealed that XEDAR is dispensable for ectodermal appendage development (Newton et al., 2004), there may be redundancy between TROY and XEDAR signalling in hair follicle development. Therefore, we analysed the expression of TROY during the most important stages of hair development.

Interestingly, TROY mRNA was not expressed at E14, when primary guard hairs develop, and at E15.5 only very weak staining was observed (Fig. 7C). But strong expression of TROY mRNA was detected at E17.5 and P0, when secondary follicles form (Fig. 7C). Expression of TROY co-localized with NF-κB activity (see Fig. 2). In $c^{I\kappa B\alpha\Delta N}$ mice, TROY expression was still observed at P0, indicating that like Eda A1, TROY is not regulated by NF-κB (data not shown). It was also expressed in the matrix of guard hair follicles at P0 (Fig. 7C). According to the expression pattern, one can deduce that TROY may be specifically involved in regulating secondary hair follicle development.

DISCUSSION

We show that NF-κB is dispensable for hair placode initiation, yet it is essential for the subsequent down growth and proliferation of hair placode keratinocytes. In addition, we demonstrate for the first time that in vivo NF-κB is activated downstream of Eda A1 and EdaR signalling. The variable requirement of NF-κB for the development of each of the four types of pelage hair follicles (see Fig. 8) underscores the emerging concept that the development of different skin appendage subtypes is regulated by differential molecular controls. Finally, we provide evidence that NF-κB-dependent hair placode down growth involves downstream induction of Shh and cyclin D1 expression.

So far it has not been known at which stage hair placode development is arrested in *tabby*, *downless* or $c^{I\kappa B\alpha\Delta N}$ mice. Our finding that primary guard hair placode development is interrupted in $c^{I\kappa B\alpha\Delta N}$ and *downless* mice at pre-placode stage 0/1, and that Eda A1/EdaR/NF-κB are not needed for placode initiation, supports data from K14-Dkk1 transgenic mice, where hair placodes fail to develop in the absence of Wnt (Andl et al., 2002). This indicates that Wnt is required for initiation of placode formation, and that Eda A1/EdaR/NF-κB is most probably activated directly downstream of the initiating Wnt signal. Furthermore, as was shown here and in a previous report (Headon and Overbeek, 1999), EdaR is still expressed ubiquitously in the epidermis at E13.5. Thus, there has to be a yet unknown signal that directs EdaR expression exclusively to hair placodes to start NF-κB signalling. Wnt is a possible candidate, as the K14-Dkk1 transgenic mice no longer revealed placodal EdaR expression at E14.5 (Andl et al., 2002).

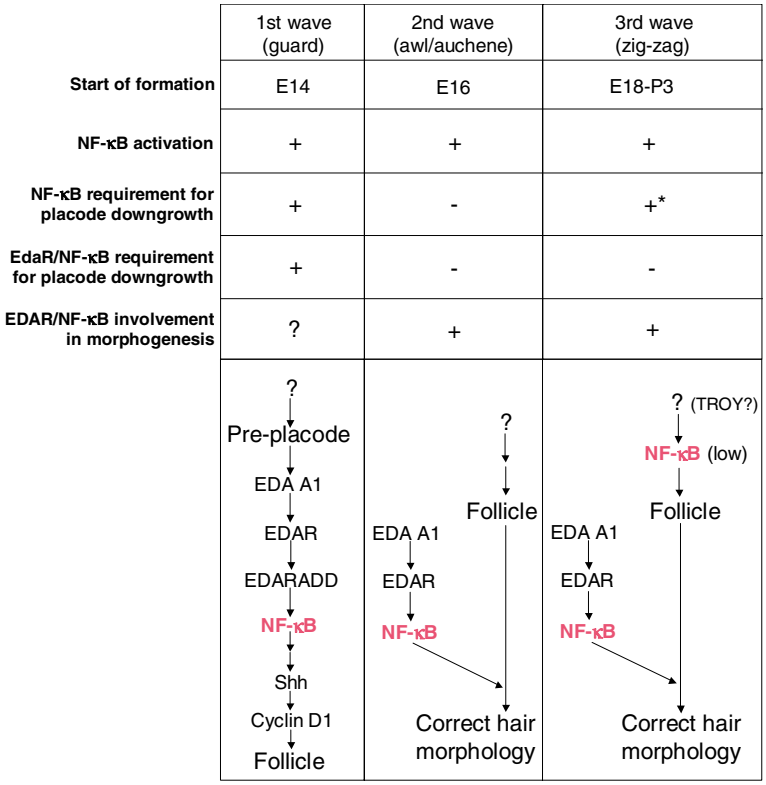

Fig. 8. Working hypothesis on the role of NF-κB in guard, zigzag or awl hair development. The upper panel displays the degree of involvement of NF-κB or EdaR/NF-κB during the development of the four pelage hair types, proceeding in three different waves. Activation of NF-κB is reflected by the X-Gal activity in the NF-κB reporter mice (*κGal*). *The NF-κB activating signal for the formation or down growth of zigzag placodes remains unknown. A possible role of EdaR/NF-κB in the morphogenesis of guard hairs has also not been identified yet (indicated by '?'). The lower scheme indicates the time point at which Eda A1/EdaR/NF-κB contribute to the development of each hair type. Shh and cyclin D1 are downstream of EdaR/NF-κB in guard hair follicles. It remains to be determined whether this is also true for zigzag follicles, and whether NF-κB directly regulates Shh.

The loss of structural placode organization observed in $c^{I\kappa B\alpha\Delta N}$ and *downless* mice may account for the previously described 'delayed epidermal differentiation' in *tabby* embryos at E14 and E15 (Laurikkala et al., 2002). The apoptotic cells we observed in the epidermis of $c^{I\kappa B\alpha\Delta N}$ and *downless* mice were localized in the suprabasal layer and the dermis, where no NF-κB activity was found. Therefore, we can conclude that NF-κB has no anti-apoptotic function downstream of Eda A1/EdaR in hair forming keratinocytes in vivo, which is in agreement with earlier results obtained from analysing *tabby* teeth (Koppinen et al., 2001).

In the current study, we asked whether NF-κB regulates keratinocyte proliferation by direct or indirect activation of cell cycle genes. Cyclin D1 was previously described as a direct NF-κB target gene in several cell types (Hinz et al., 1999), but in vascular smooth muscle cells, for example, cyclin D1 is not activated by NF-κB (Mehrhof et al., 2005). Analysis of the temporal expression pattern of the G1 phase regulator, cyclin D1, in placodal keratinocytes revealed that upregulation did not take place until developmental stages 2-3, and, hence, correlated with Shh upregulation. Thus, hair placode keratinocytes may be another example where cyclin D1 is not directly regulated by NF-κB. Furthermore, cyclin D1 expression is entirely independent of NF-κB activity in awl hairs (data not shown). In this hair type, Eda A1/EdaR/NF-κB is neither required for placode formation and subsequent down growth, nor for mature follicle development, but is needed to determine the ultrastructure of the hair.

Our data suggest that cyclin D1 is more likely to be induced by Shh and/or Wnt10b signalling, which are both downstream of Eda A1/NF-κB activation (R. Schmidt-Ullrich, unpublished) (Andl et al., 2002; Laurikkala et al., 2002). Furthermore, Shh has previously been shown to be essential for cyclin D1 expression (Mill et al., 2003). Although Shh expression does not appear until stage 1 of hair follicle morphogenesis and is described as a target gene of β-catenin (Gat et al., 1998; Huelsken et al., 2001), Eda A1/NF-κB may directly regulate epidermal Wnt10b expression, as placodal Wnt10b expression is also absent in *tabby* mice at E14.5 (Andl et al., 2002). Because expression of cyclin D1 can already be weakly detected in stage 1 placodes, there may also be synergy between Eda A1/EdaR/NF-κB, Shh and Wnt signalling that results in a strong growth signal. The identification of specific target genes of NF-κB in hair placodes may answer this question.

Analysis of *κGal* × *tabby* mice has helped to demonstrate the necessity of NF-κB in guard hair follicle development: skin explants from these mice showed that classical signals inducing NF-κB activity, although not physiologically relevant for hair placode formation like TNFα and PMA, can regenerate placodes at E13.5 + 1 day. These results clearly reveal NF-κB as an essential promoter of guard hair placode growth. After TNFα, and to a lesser degree after Eda A1, treatment of *tabby* × *κGal* explants, X-Gal staining was also observed in interfollicular keratinocytes (see Fig. 6). Thus, theoretically, NF-κB can be activated anywhere in the epidermis if the right signal appears. However, the Shh probe only marked hair placodes. Therefore, Shh is downstream of NF-κB in those epidermal keratinocytes that previously must have been programmed for hair placode fate in *κGal* × *tabby* mice at E13.5. The programming most probably includes a generally permissive signal (i.e. 'make an appendage'), which was previously proposed to be dermal, and which may facilitate the formation of gradients of placode activators versus inhibitors defining placode borders (Hardy, 1992). This is in agreement with our finding that some placode initiation processes have already taken place in *tabby*, *downless* and $c^{I\kappa B\alpha\Delta N}$ mice.

NF-κB activity and EdaR expression were detected in all hair types, including secondary awls and vibrissae. The bona fide development of awl hairs and most vibrissae types is independent of NF-κB activity, because it is not affected in $c^{I\kappa B\alpha\Delta N}$, *tabby*, *downless*

or *crinkled* mice (Gruneberg, 1971; Headon et al., 2001; Schmidt-Ullrich et al., 2001) (see also Fig. 5A, right panel). Hence, EdaR/NF-κB activity would not be expected in these hair types. However, awl hairs do have a slightly abnormal shape in all these mice, suggesting that Eda A1/EdaR/NF-κB regulate the correct ultrastructure (see Fig. 8) (Falconer, 1952; Schmidt-Ullrich et al., 2001). Moreover, mammary glands, which also exhibit strong embryonic NF-κB activity, develop and function normally in $c^{I\kappa B\alpha\Delta N}$ mice, even though nipple morphology is altered as in *tabby* mice (data not shown) (Mustonen et al., 2003). Eda A1 and EdaR are expressed and active not only in mammals, but also in bird feather tracts and fish scales (Houghton et al., 2005; Kondo et al., 2001; Pispa and Thesleff, 2003; Sharpe, 2001; Thesleff and Mikkola, 2002). In the Japanese fish medaka (*Oryzias latipes*), for example, it was discovered that the rs-3 (reduced scale-3) locus encodes EdaR (Kondo et al., 2001). Fish with mutations in rs-3 completely lack scales (Kondo et al., 2001). Thus, in vertebrates, Eda A1/EdaR/NF-κB signalling is required for the development and shaping of ectodermal appendages, which suggests that it is an evolutionary conserved pathway. However, this appears to have become redundant for the development of some mammalian appendages such as awl hairs, vibrissae or mammary glands.

Complete lack of secondary zigzag hairs in $c^{I\kappa B\alpha\Delta N}$ mice also points to an important role of NF-κB in the development of this pelage hair type (Fig. 7). In part, zigzag hair development depends on Eda A1/EdaR signalling, because *tabby* and *downless* mice also do not develop proper zigzag hairs (Gruneberg, 1971; Vielkind and Hardy, 1996). But rescue experiments in *tabby* mice reveal that transgenic Eda A1 expression only reconstitutes guard and not zigzag hair follicles (Cui et al., 2003; Gaide and Schneider, 2003). Furthermore, it is noteworthy that in wild-type mice, Eda A1 overexpression in epidermal keratinocytes equally leads to the absence of zigzag hairs (Mustonen et al., 2003). Thus, the dose of Eda A1 signalling and its spatial distribution need to be controlled by yet unknown factors in order to form normal zigzag hairs. Importantly, *tabby* mice develop abnormal awl instead of zigzag hairs, resulting in almost wild-type hair numbers (Cui et al., 2003). This is in contrast to $c^{I\kappa B\alpha\Delta N}$ mice and strongly suggests that NF-κB activation downstream of Eda A1 alone is not sufficient to develop complete zigzag hair follicles. This is also supported by our finding of residual NF-κB activity in many secondary hair placodes of *tabby* and *downless* × *κGal* mice at P0. The orphan TNF receptor TROY was first expressed at E17, hinting that perhaps both TROY and Eda A1/EdaR are needed to form zigzag hairs via NF-κB (see Fig. 8). Owing to possible redundancy, one cannot exclude that XEDAR and other NF-κB activators are also involved. In such a scenario, residual EdaR-independent NF-κB activity originating from TROY, XEDAR or other NF-κB activators was predicted to occur in early secondary hair placodes of *tabby* and *downless* mice (see Fig. 5B).

The ability to develop awl instead of zigzag hairs in *tabby* mice suggests that the initiating developmental pathways leading to both pelage hair types are identical, depending on Noggin, Lef1, BMP and Wnt (Botchkarev et al., 1999; Botchkarev et al., 2002; Jamora et al., 2003; Schmidt-Ullrich and Paus, 2005). However, the subsequent regulation of the morphological ultrastructure of zigzags, such as the two 'kinks', seem to be regulated specifically by Eda A1/EdaR/NF-κB (see Fig. 8). Molar tooth development presents yet another example where Eda A1/EdaR/NF-κB signalling regulates the morphogenesis of cusps (Ohazama et al., 2004b). Thus, in ectodermal appendage development the specific role of NF-κB depends on the type of appendage, and controls either early developmental or later morphogenetic processes.

We have provided a comprehensive analysis of the differential functional requirement and the spatial and temporal activation of NF-κB during primary and secondary hair follicle development. We further presented a genetically based dissection of the integration of NF-κB within upstream (Eda A1, EdaR) and downstream (Shh, cyclin D1) signalling modules and genes. This will be the basis for future analysis of gene networks that are under direct control of NF-κB, and of the mechanisms that determine redundancy with NF-κB-independent pathways in epidermal appendage ontogeny.

We thank Karin Ganzel and Sarah Ugowski for excellent technical help, and Gundula Pilnitz-Stolze (Hautklinik UKE, Universität Hamburg, Hamburg, Germany) for performing the immunohistochemistry in Fig. 1C. The authors also thank Joerg Huelsken for providing the downless, Shh and tabby probes; Atsushi Ohazama (Showa University Dental School, Tokyo, Japan) for providing the TROY probe; Gregory Shackleford for providing the Wnt10a and Wnt10b probes; and Irma Thesleff for providing *tabby* mice. This work was supported in part by a BMBF grant to C.S.

References

Aggarwal, B. B. (2003). Signalling pathways of the TNF superfamily: a double-edged sword. *Nat. Rev. Immunol.* **3**, 745-756.
Andl, T., Reddy, S. T., Gaddapara, T. and Millar, S. E. (2002). WNT signals are required for the initiation of hair follicle development. *Dev. Cell* **2**, 643-653.
Barton, D., HogenEsch, H. and Weih, F. (2000). Mice lacking the transcription factor RelB develop T cell-dependent skin lesions similar to human atopic dermatitis. *Eur. J. Immunol.* **30**, 2323-2332.
Botchkarev, V. A., Botchkareva, N. V., Roth, W., Nakamura, M., Chen, L. H., Herzog, W., Lindner, G., McMahon, J. A., Peters, C., Lauster, R. et al. (1999). Noggin is a mesenchymally derived stimulator of hair-follicle induction. *Nat. Cell. Biol.* **1**, 158-164.
Botchkarev, V. A., Botchkareva, N. V., Sharov, A. A., Funa, K., Huber, O. and Gilchrest, B. A. (2002). Modulation of BMP signaling by noggin is required for induction of the secondary (nontylotrich) hair follicles. *J. Invest. Dermatol.* **118**, 3-10.
Cui, C. Y., Durmowicz, M., Ottolenghi, C., Hashimoto, T., Griggs, B., Srivastava, A. K. and Schlessinger, D. (2003). Inducible mEDA-A1 transgene mediates sebaceous gland hyperplasia and differential formation of two types of mouse hair follicles. *Hum. Mol. Genet.* **12**, 2931-2940.
Falconer, D. S. (1952). A totally sex-linked gene in the house mouse. *Nature* **169**, 664-665.
Gaide, O. and Schneider, P. (2003). Permanent correction of an inherited ectodermal dysplasia with recombinant EDA. *Nat. Med.* **9**, 614-618.
Gat, U., DasGupta, R., Degenstein, L. and Fuchs, E. (1998). De Novo hair follicle morphogenesis and hair tumors in mice expressing a truncated beta-catenin in skin. *Cell* **95**, 605-614.
Gruneberg, H. (1971). The tabby syndrome in the mouse. *Proc. R. Soc. Lond. B Biol. Sci.* **179**, 139-156.
Hardy, M. H. (1992). The secret life of the hair follicle. *Trends Genet.* **8**, 55-61.
Hayden, M. S. and Ghosh, S. (2004). Signaling to NF-κB. *Genes Dev.* **18**, 2195-2224.
Headon, D. J. and Overbeek, P. A. (1999). Involvement of a novel Tnf receptor homologue in hair follicle induction. *Nat. Genet.* **22**, 370-374.
Headon, D. J., Emmal, S. A., Ferguson, B. M., Tucker, A. S., Justice, M. J., Sharpe, P. T., Zonana, J. and Overbeek, P. A. (2001). Gene defect in ectodermal dysplasia implicates a death domain adapter in development. *Nature* **414**, 913-916.
Hinz, M., Krappmann, D., Eichten, A., Heder, A., Scheidereit, C. and Strauss, M. (1999). NF-κB function in growth control: regulation of cyclin D1 expression and G0/G1-to-S-phase transition. *Mol. Cell. Biol.* **19**, 2690-2698.
Houghton, L., Lindon, C. and Morgan, B. A. (2005). The ectodysplasin pathway in feather tract development. *Development* **132**, 863-872.
Hu, Y., Baud, V., Oga, T., Kim, K. I., Yoshida, K. and Karin, M. (2001). IKK· controls formation of the epidermis independently of NF-κB. *Nature* **410**, 710-714.
Huelsken, J., Vogel, R., Erdmann, B., Cotsarelis, G. and Birchmeier, W. (2001). α-Catenin controls hair follicle morphogenesis and stem cell differentiation in the skin. *Cell* **105**, 533-545.
Jamora, C., DasGupta, R., Kocieniewski, P. and Fuchs, E. (2003). Links between signal transduction, transcription and adhesion in epithelial bud development. *Nature* **422**, 317-322.
Karin, M. and Ben-Neriah, Y. (2000). Phosphorylation meets ubiquitination: the control of NF-κB activity. *Annu. Rev. Immunol.* **18**, 621-663.
Karnovsky, M. (1965). Formaldehyde-glutaraldehyde fixative of high osmolarity for use in electron microscopy. *Histopathology* **27**, 137-138.
Kojima, T., Morikawa, Y., Copeland, N. G., Gilbert, D. J., Jenkins, N. A., Senba, E. and Kitamura, T. (2000). TROY, a newly identified member of the

tumor necrosis factor receptor superfamily, exhibits a homology with EdaR and is expressed in embryonic skin and hair follicles. *J. Biol. Chem.* **275**, 20742-20747.

Kondo, S., Kuwahara, Y., Kondo, M., Naruse, K., Mitani, H., Wakamatsu, Y., Ozato, K., Asakawa, S., Shimizu, N. and Shima, A. (2001). The medaka rs-3 locus required for scale development encodes ectodysplasin-A receptor. *Curr. Biol.* **11**, 1202-1206.

Koppinen, P., Pispa, J., Laurikkala, J., Thesleff, I. and Mikkola, M. L. (2001). Signaling and subcellular localization of the TNF receptor EdaR. *Exp. Cell Res.* **269**, 180-192.

Krappmann, D., Wulczyn, F. G. and Scheidereit, C. (1996). Different mechanisms control signal-induced degradation and basal turnover of the NF-κB inhibitor IκBα in vivo. *EMBO J.* **15**, 6716-6726.

Kumar, A., Eby, M. T., Sinha, S., Jasmin, A. and Chaudhary, P. M. (2001). The ectodermal dysplasia receptor activates the nuclear factor-κB, JNK, and cell death pathways and binds to ectodysplasin A. *J. Biol. Chem.* **276**, 2668-2677.

Laurikkala, J., Pispa, J., Jung, H. S., Nieminen, P., Mikkola, M., Wang, X., Saarialho-Kere, U., Galceran, J., Grosschedl, R. and Thesleff, I. (2002). Regulation of hair follicle development by the TNF signal ectodysplasin and its receptor EdaR. *Development* **129**, 2541-2553.

Le Bail, O., Schmidt-Ullrich, R. and Israel, A. (1993). Promoter analysis of the gene encoding the IκB-α/MAD3 inhibitor of NF-κB: positive regulation by members of the rel/NF-kappa B family. *EMBO J.* **12**, 5043-5049.

Mehrhof, F. B., Schmidt-Ullrich, R., Dietz, R. and Scheidereit, C. (2005). Regulation of vascular smooth muscle cell proliferation: role of NF-κB revisited. *Circ. Res.* **96**, 958-964.

Mikkola, M. L., Pispa, J., Pekkanen, M., Paulin, L., Nieminen, P., Kere, J. and Thesleff, I. (1999). Ectodysplasin, a protein required for epithelial morphogenesis, is a novel TNF homologue and promotes cell-matrix adhesion. *Mech. Dev.* **88**, 133-146.

Mill, P., Mo, R., Fu, H., Grachtchouk, M., Kim, P. C., Dlugosz, A. A. and Hui, C. C. (2003). Sonic hedgehog-dependent activation of Gli2 is essential for embryonic hair follicle development. *Genes Dev.* **17**, 282-294.

Millar, S. E. (2002). Molecular mechanisms regulating hair follicle development. *J. Invest. Dermatol.* **118**, 216-225.

Mustonen, T., Pispa, J., Mikkola, M. L., Pummila, M., Kangas, A. T., Pakkasjarvi, L., Jaatinen, R. and Thesleff, I. (2003). Stimulation of ectodermal organ development by Ectodysplasin-A1. *Dev. Biol.* **259**, 123-136.

Mustonen, T., Ilmonen, M., Pummila, M., Kangas, A. T., Laurikkala, J., Jaatinen, R., Pispa, J., Gaide, O., Schneider, P., Thesleff, I. et al. (2004). Ectodysplasin A1 promotes placodal cell fate during early morphogenesis of ectodermal appendages. *Development* **131**, 4907-4919.

Naito, A., Yoshida, H., Nishioka, E., Satoh, M., Azuma, S., Yamamoto, T., Nishikawa, S. and Inoue, J. (2002). TRAF6-deficient mice display hypohidrotic ectodermal dysplasia. *Proc. Natl. Acad. Sci. USA* **99**, 8766-8771.

Newton, K., French, D. M., Yan, M., Frantz, G. D. and Dixit, V. M. (2004). Myodegeneration in EDA-A2 transgenic mice is prevented by XEDAR deficiency. *Mol. Cell. Biol.* **24**, 1608-1613.

Ohazama, A., Courtney, J. M., Tucker, A. S., Naito, A., Tanaka, S., Inoue, J. and Sharpe, P. T. (2004a). Traf6 is essential for murine tooth cusp morphogenesis. *Dev. Dyn.* **229**, 131-135.

Ohazama, A., Hu, Y., Schmidt-Ullrich, R., Cao, Y., Scheidereit, C., Karin, M., Sharpe, P. T., Courtney, J. M., Tucker, A. S., Naito, A. et al. (2004b). A dual role for IKKα in tooth development. *Dev. Cell* **6**, 219-227.

Pasparakis, M., Courtois, G., Hafner, M., Schmidt-Supprian, M., Nenci, A., Toksoy, A., Krampert, M., Goebeler, M., Gillitzer, R., Israel, A. et al. (2002). TNF-mediated inflammatory skin disease in mice with epidermis-specific deletion of IKK2. *Nature* **417**, 861-866.

Paus, R., Muller-Rover, S., Van Der Veen, C., Maurer, M., Eichmuller, S., Ling, G., Hofmann, U., Foitzik, K., Mecklenburg, L. and Handjiski, B. (1999). A comprehensive guide for the recognition and classification of distinct stages of hair follicle morphogenesis. *J. Invest. Dermatol.* **113**, 523-532.

Philpott, M. P. and Paus, R. (1998). Principles of hair follicle morphogenesis. In *Molecular Basis of Epithelial Appendage Morphogenesis* (ed. C.-M. Chuong), pp. 75-103. Austin (TX): Landes Bioscience.

Pispa, J. and Thesleff, I. (2003). Mechanisms of ectodermal organogenesis. *Dev. Biol.* **262**, 195-205.

Schmidt-Ullrich, R. and Paus, R. (2005). Molecular principles of hair follicle induction and morphogenesis. *BioEssays* **27**, 247-261.

Schmidt-Ullrich, R., Memet, S., Lilienbaum, A., Feuillard, J., Raphael, M. and Israel, A. (1996). NF-κB activity in transgenic mice: developmental regulation and tissue specificity. *Development* **122**, 2117-2128.

Schmidt-Ullrich, R., Aebischer, T., Hulsken, J., Birchmeier, W., Klemm, U. and Scheidereit, C. (2001). Requirement of NF-κB/Rel for the development of hair follicles and other epidermal appendices. *Development* **128**, 3843-3853.

Sharpe, P. T. (2001). Fish scale development: Hair today, teeth and scales yesterday? *Curr. Biol.* **11**, R751-R752.

St-Jacques, B., Dassule, H. R., Karavanova, I., Botchkarev, V. A., Li, J., Danielian, P. S., McMahon, J. A., Lewis, P. M., Paus, R. and McMahon, A. P. (1998). Sonic hedgehog signaling is essential for hair development. *Curr. Biol.* **8**, 1058-1068.

Sundberg, J. P. (1994). *Handbook of Mouse Mutations with Skin and Hair Abnormalities: Animal Models and Biomedical Tools.* Boca Raton (FL): CRC Press.

Thesleff, I. and Mikkola, M. L. (2002). Death receptor signaling giving life to ectodermal organs. *Sci. STKE* **2002**, E22.

Tobin, D. J., Fenton, D. A. and Kendall, M. D. (1990). Ultrastructural observations on the hair bulb melanocytes and melanosomes in acute alopecia areata. *J. Invest. Dermatol.* **94**, 803-807.

Tobin, D. J., Fenton, D. A. and Kendall, M. D. (1991). Cell degeneration in alopecia areata. An ultrastructural study. *Am. J. Dermatopathol.* **13**, 248-256.

Vielkind, U. and Hardy, M. H. (1996). Changing patterns of cell adhesion molecules during mouse pelage hair follicle development. 2. Follicle morphogenesis in the hair mutants, Tabby and downy. *Acta Anat. (Basel)* **157**, 183-194.

Yan, M., Wang, L. C., Hymowitz, S. G., Schilbach, S., Lee, J., Goddard, A., de Vos, A. M., Gao, W. Q. and Dixit, V. M. (2000). Two-amino acid molecular switch in an epithelial morphogen that regulates binding to two distinct receptors. *Science* **290**, 523-527.